

An Ultra-Wideband Modified Vivaldi Antenna Applied to Ground and Through the Wall Imaging

Ziani Tahar^{1, *}, Xavier Dérobert², and Malek Benslama³

Abstract—In this paper, we are interested in the design of a new Ultra-Wideband (UWB) directional Vivaldi antenna with narrow beam, in the frequency range of 1.17 to 4.75 GHz. The simulation of the designed antenna is carried out on Computer Simulation Technology Microwave Studio (CST-MWS). The mutual coupling effect reduction is considered. The designed antenna is tested for Ground Penetrating Radar (GPR) and Through the Wall applications. The emitted waveform is a Stepped Frequency Continuous Wave (SFCW) signal, generated by a Vector Network Analyser (VNA). The acquired raw data are focused by using back projection algorithm.

1. INTRODUCTION

Any antenna working in a spectrum occupying a bandwidth greater than 20% of the center frequency or having a bandwidth greater than 500 MHz is defined as an Ultra-Wideband (UWB) one [1]. An increasing demand for UWB antenna is noticed for different applications such as communication [1, 2] and radar imaging [3–6]. The antennas for such applications must be compact and lightweight for portability. Besides their compact size, they must have a stable gain and low cross polarization.

It is known that more bandwidth is increased, and more resolution is improved, but this resolution depended on which application we wanted. For example, using ground penetrating radar (GPR) technique, wide bandwidth must be thought with care because higher frequencies are more attenuated by soil than lower ones [7–9].

In GPR mines detection, targets are located in the upper depth of soil. In this case, an antenna must have a wider bandwidth and a narrower beam for high spatial resolution. Nevertheless, this technique is limited in the high frequencies (central frequencies about 2.5–3 GHz).

A complementary innovative technique is the step-frequency radar (SFR) using a vector network analyser (VNA) with a UWB antenna in very high frequencies, above GPR ones. Thus, the spatial resolution, combined with a better signal to noise ratio, enables to promote better performances of sub-surface civil engineering applications. Higher frequency band enables to survey very thin road layers [10], limestone walls of historical buildings [11] or sub-surface soil [12] for moisture estimation. In these last examples, the antennas associated with the SFR techniques were UWB air-coupled antennas, working as dipoles, which enable to model the radar propagation and then perform the full-wave form inversion technique to reconstruct the surveyed geometries quantitatively.

One kind of such UWB antennas meeting these characteristics is Vivaldi antenna. After it was presented first by Gibson [13] and then modified to a tapered slot antenna by Lewis et al. [14], Vivaldi antenna was widely applied in different applications [1, 5, 6].

Vivaldi antenna has many advantages such as simple structure, low cost design, high stable gain and a UWB. It also provides a smooth transition between the guided wave travelling in the transmission line and a plane wave which is radiated.

Received 15 May 2018, Accepted 16 July 2018, Scheduled 14 August 2018

* Corresponding author: Ziani Tahar (ziani1_tahar1@gmail.com).

¹ EMP, Bordj El Bahri, Algiers, Algeria. ² IFSTTAR, Nantes, France. ³ University of Constantine, Algeria.

Vivaldi antennas are planar antennas that work over a wide frequency range. They provide a medium gain depending on length of the taper and shape of the curvature. The gain is varied with frequency and generally situated between 4 dBi and 8 dBi. Vivaldi antennas could be used with both multi-band and impulse technologies. They offer wide bandwidth characteristics and produce symmetrical radiation pattern in H -plane and E -plane. Their bandwidth can be changed by varying antenna parameters such as shape, length, dielectric constant and dielectric thickness.

When being used for pulse technologies like radar, Vivaldi antennas have a high peak value for the pulse envelope. They offer stable group delay and allow for a narrow pulse width. Vivaldi antennas can be fed with a signal directly from a strip, which also allows them to work in phased array applications.

The design of Vivaldi antenna is simple compared to log periodic and fractal antenna designs. However, they suffer from some drawbacks such as low or inconsistent gain and directivity for only balanced antipodal antenna case (for this a dielectric lens is added) [15]. The lens tends to limit their wide spread utilization. They are costlier due to complex fabrication process. Especially for manufacturing of a balanced antipodal Vivaldi antenna which is more complex due to its tri-plate structure. Another disadvantage as majority of antennas is applying directly formulas given in Section 2.1. So, we could not satisfy our needs in terms of gain, desired return loss and narrow beam without modifying the antenna like adding circular slots or/and linear slots if it is necessary to perform it.

In our work, optimisations were done to improve antenna performances for GPR sub-surface applications and through the wall imaging, focusing on a depth penetration about 1–1.5 m, a high resolution combined with narrow beam.

As the first step the Vivaldi antenna, as given in [16, 17], was studied and then modified in order to improve its performances reaching our objectives. Several numerical parametric studies were performed in order to design an evolution of the antenna, integrating a change in the opening rate of the slot taper and by adding circular and linear slots.

In the second step, a special care is given for the study of the mutual coupling effect (called S_{21} coefficient) between two antennas, when using a bistatic mode (emitting/receiving configuration) with a constant offset.

Last part of the paper is devoted to experimental campaigns in controlled laboratory configuration, while embedding metallic reflector corners and plastic cylinders, completed for the last experiments by a masonry wall.

The work presented in this paper is organized as follows. Section 2 gives the new modified Vivaldi antenna design and its performances. Section 3 summarizes experimental measures for GPR detection in soil and through the wall. Section 4, concludes work's paper.

2. DESIGN OF AN ULTRA-WIDEBAND MODIFIED VIVALDI ANTENNA

2.1. Vivaldi Antenna

The design of Vivaldi antenna consists of an exponentially tapered slot cut in a metal film designed on a low cost FR4 substrate with dielectric constant permittivity $\epsilon_r = 4.3$, thickness $h = 1.5$ mm and loss tangent $\delta = 0.025$. It flares from 50Ω to a large opening notch. The Vivaldi antenna must have [16, 17]:

- A length (L), greater than a half of wavelength ($\lambda/2$), where $\lambda = c/f$; c is the light speed, and f can have two values, f_{\min} and f_{\max} of the bandwidth (we can calculate λ_{\max} by taking f_{\min} and λ_{\min} by taking f_{\max}). So, L is greater than 15.7 cm.
- A wide (W), greater than a quarter of wavelength ($\lambda/4$). So, it is greater than 7.85 cm.
- A circular cavity diameter (D), equal to a quarter of the guide wavelength in the slot line (free space) at the center operating frequency of the antenna ($f_0 = 2.96 \approx 3$ GHz). In our case it is equal to 2.4 cm.

However, for other authors [17], antenna is dimensioned as follows (see Figure 1) by Equation (1) which gives both length and width at the lowest operating frequency of the antenna f_{\min} as:

$$L = W = \frac{c}{f_{\min}} \sqrt{\frac{2}{\epsilon_r + 1}} \quad (1)$$

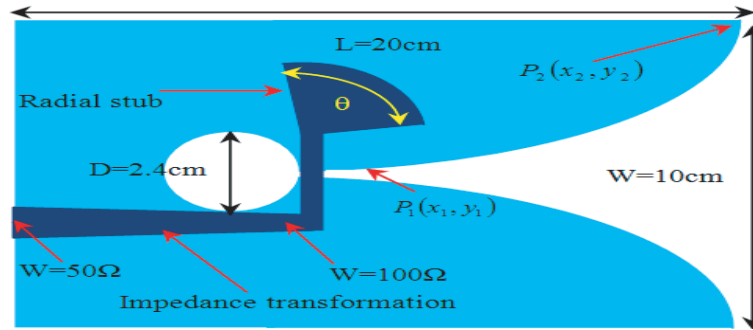


Figure 1. Vivaldi antenna (in front view) and its feeding line (in back view).

The exponential curve of Vivaldi antenna is defined by Equations (2), (3) and (4) as:

$$Y = C_1 e^{ax} + C_2 \tag{2}$$

where C_1 and C_2 are given by:

$$C_1 = \frac{y_2 - y_1}{e^{ax_2} - e^{ax_1}} \tag{3}$$

$$C_2 = \frac{e^{ax_2} y_1 - e^{ax_1} y_2}{e^{ax_2} - e^{ax_1}} \tag{4}$$

Here, C_1 and C_2 are constants, and ‘a’ is the opening rate of the exponential taper. x_1, x_2, y_1 and y_2 indicate the slot line start-end points. We can give the representation of Vivaldi antenna and its feeding line in Figure 1.

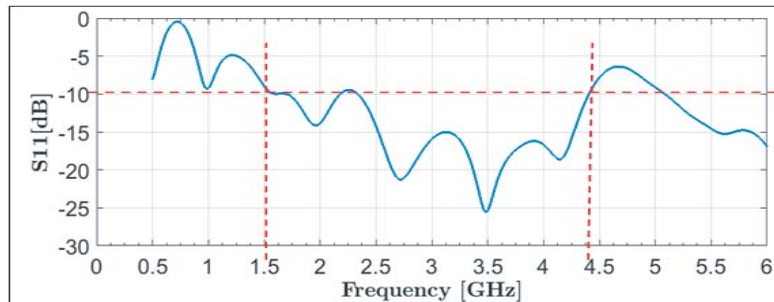


Figure 2. Return loss (S_{11}) response of Vivaldi antenna before optimization.

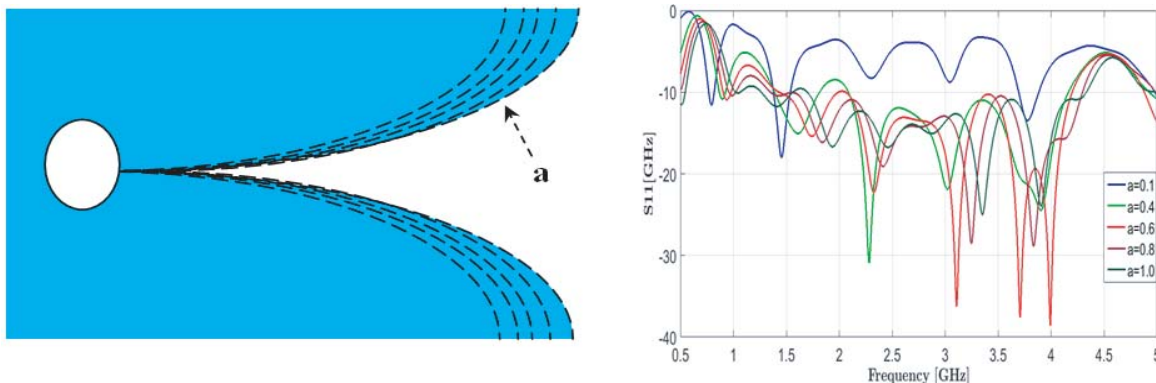


Figure 3. Influence of opening rate exponential taper a .

The S_{11} result of simulation obtained with CST software is given by Figure 2.

From the result given in Figure 2, we can notice that S_{11} does not meet our objectives, as the antenna is capable of achieving an impedance adaptation from only 2.3 to 4.4 GHz, and the frequency range from 1 to 1.5 GHz is higher than -10 dB.

That is why a study to obtain our requirements is necessary while modifying the shape of Vivaldi antenna. The following parametric study focuses on the modification of the opening rate of the slot taper and the adding of circular and linear slots.

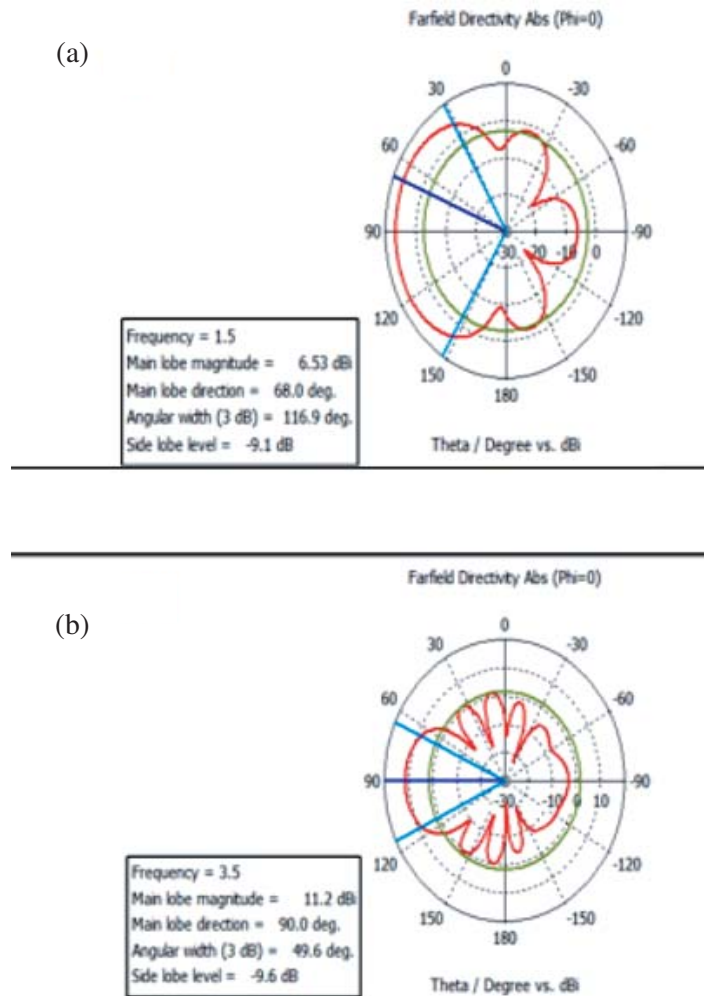


Figure 4. Beam and gain of antenna for (a) $f = 1.5$ and (b) $f = 3.5$ GHz.

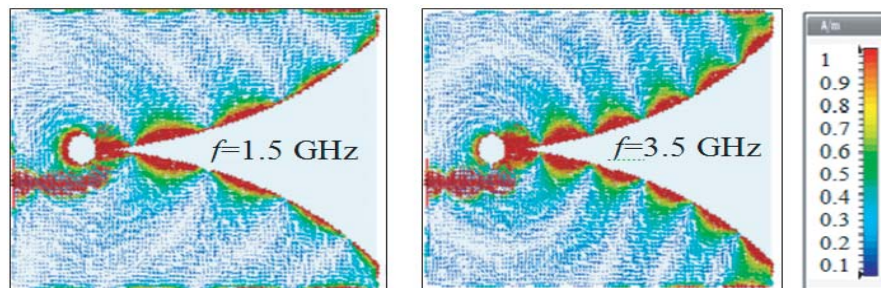


Figure 5. Current density for $f = 1.5$ and $f = 3.5$ GHz.

2.2. Performance Study

The first investigation is made on varying the coefficient a (opening rate of the exponential taper), and Figure 3 shows the simulation of S_{11} when taking the dimensions given in Figure 1 and using an optimum value (return loss ≤ -10 dB) as reference because the electromagnetic wave being transmitted is more than 90% of the injected signal. It gave a lower value of S_{11} .

To make more optimizations, slot or/and lines must be added, knowing that there are no formulas for calculating line and circular slots, except for the circular cavity. Before that, we wanted first to see the intensity of surface current on the metal part (top view of antenna) and in addition, the beam for two frequencies belonging to the bandwidth [1, 3, 21, 22]. Results are shown in Figures 4 and 5.

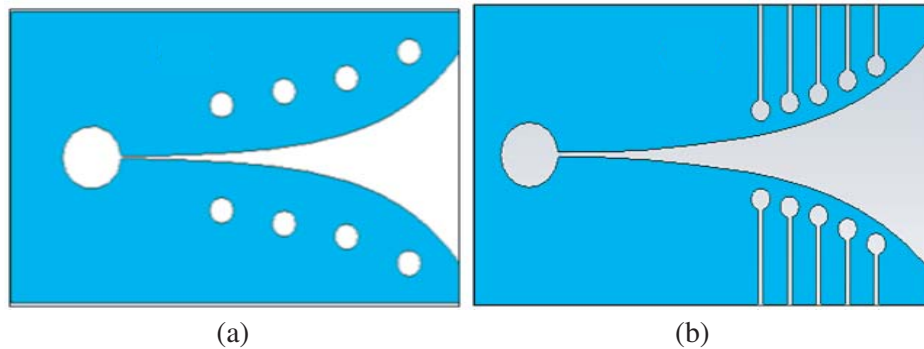


Figure 6. Vivaldi antenna by adding slot circles to the metal in (a) and Vivaldi antenna by adding slot circles and lines in (b).

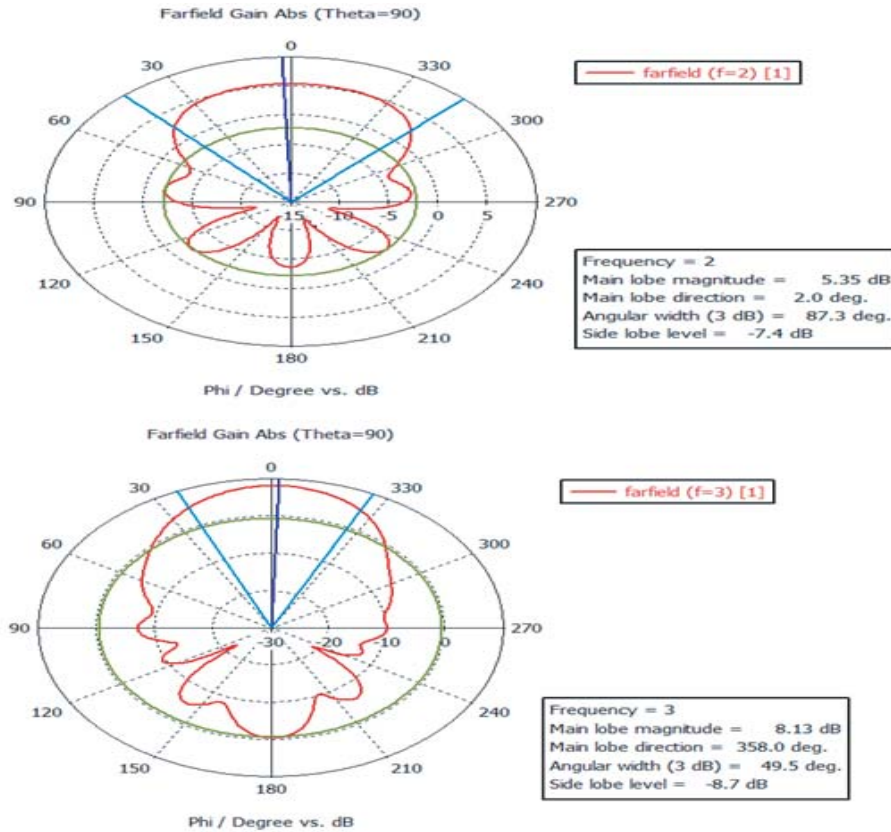


Figure 7. Beam and gain of Vivaldi antenna by adding slot circles.

It is clear from Figure 5 that some part of the antenna could be cut not randomly but in the location where current was weak. In addition, the beams represented in Figure 4 for the chosen frequencies were wide (90° for $f = 3.5$ GHz). More optimizations are necessary to reduce the width of the radiation pattern.

When adding circular slots or/and corrugations to antenna, the radiation beam of the antenna becomes narrower. However, optimizations could always be added in order to arrive at the narrowest possible beam. We took two antennas. For the first, we put a circular slot, and for the second, we add slot lines as shown in Figure 6. The results are given in Figures 7 and 8. From these figures, performances of the antenna are clearly enhanced.

We have tried to see influences of circular cavity D , in Figure 9, and it shown that value of 2.4 cm was very adapted for our antenna performance [17, 18].

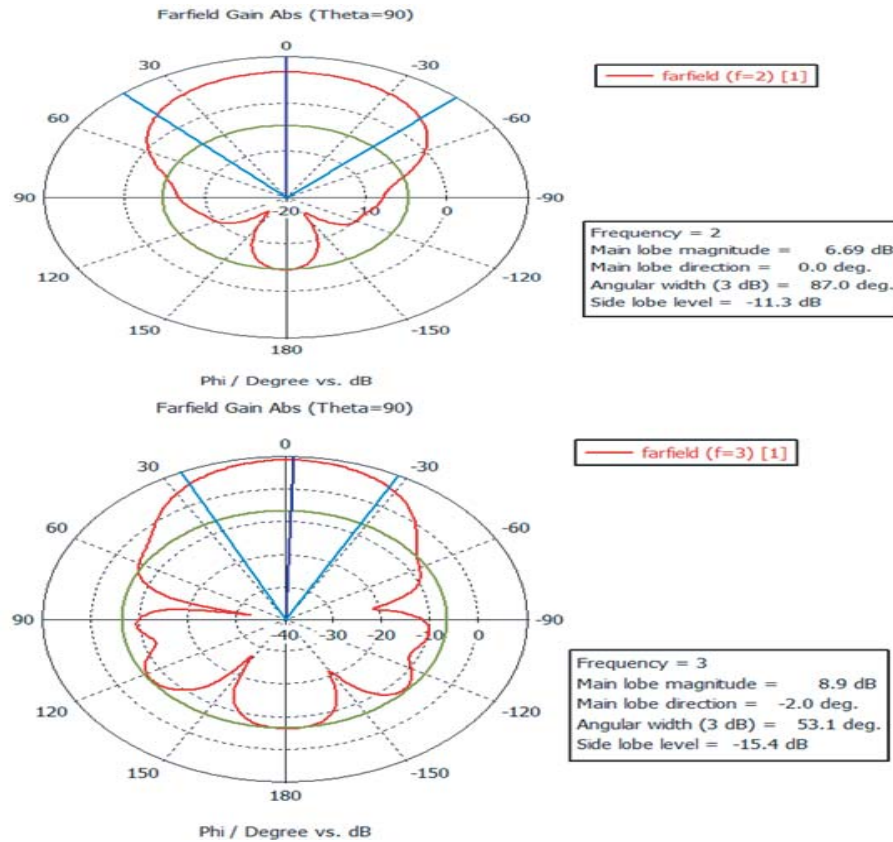


Figure 8. Beam and gain of Vivaldi antenna by adding slot circles and lines.

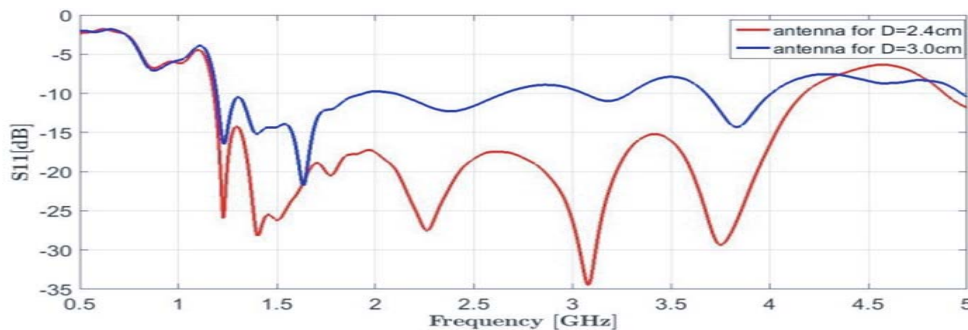


Figure 9. Influence of circular cavity.

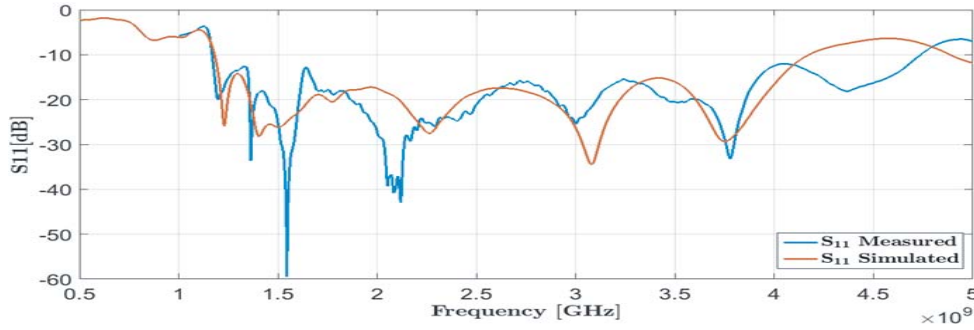


Figure 10. Return loss S_{11} in dB.

Finally, we ended up with a new antenna represented in Figure 10. The use of the radial/circular stubs feeding has been considered to achieve a large bandwidth compared to uniform stubs. The antenna is modified. Then positions of circular slots and their dimensions are modified to obtain the final dimensions. Finally, we ended up with a new antenna with: $L = 19$ cm, $W = 11$ cm and $D = 2.4$ cm.

2.3. Simulation of the New Antenna

To quantify performances of our modified Vivaldi antenna design, we need first to compare S_{11} from simulation (using CST) and measurement (using VNA). For this point we show, in Figure 11, that good agreement was obtained between measured and simulated reflection coefficients. The little difference between simulated and measured S_{11} may come from the connection loss between the printed circuit board and SMA connector.

Beam and gain simulation for our modified designed antenna are given in Figure 11. We notice that

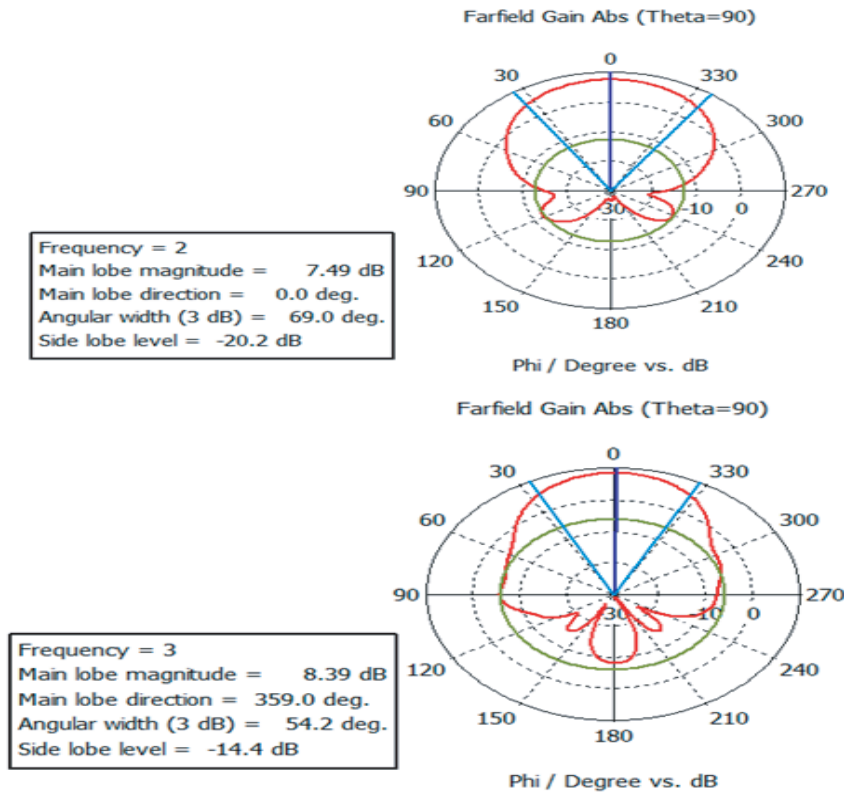


Figure 11. The designed antenna beams for two frequencies 2 and 3 GHz.

two adjacent targets at the same depth must be separated by at least one beamwidth to be distinguished as two objects. The horizontal resolution is increased when the beams become narrower [23]. We will give more details about S_{21} in Section 2.4.

From Figure 11, we show both gain and beam of the realized antenna for two frequencies, 2 and 3 GHz. These two parameters are very adapted to measurement. The gain reached 8.39 dB with a narrower beam. The antenna has a wide frequency bandwidth and directive radiation pattern.

2.4. Mutual Coupling Effect

As GPR and SFR techniques use bistatic modes most of the time, it is important to study mutual coupling effect due to the direct transmission between the antennas. S_{21} or S_{12} represents transmission from port where the signal is injected to the other port. Here, induced current will change due to the fields set up by the other port of antenna. The simple solution to reduce correlation is through physical separation between antennas. However, this solution is impractical in hand-held wireless devices considering space limitation constraints.

In our case, an alternative method to reduce mutual coupling between antennas is by putting a shift in phases where the receiver antenna is perpendicular to emitter antenna. Some positions are shown and discussed.

According to [20], the authors studied the effect of mutual coupling between multiple antennas on the outage capacity of a 2×2 Multiple-Input Multiple-Output (MIMO) system in flat fading channels. They advised a minimal loss in capacity when antennas are spaced about one wavelength.

Our objective of studying the coupling effect is to reduce the interference between antennas (known as S_{21} coefficient); for this purpose, we have put the receiving and emitting antennas in parallel or with 90° between them. We knew that when the antennas were near each other, a strong mutual coupling would exist between them which could affect the detection [24]. To solve this problem, we simulate the measurement of coefficient S_{21} of the receiving antenna which is not powered. In our study, we want to minimize coupling effects as much as possible, which exists between the two antennas and the secondary lobe with respect to the main one. For this purpose, we have from the right of Figure 12:

- (a): The two antennas are in the same plane (HH).
- (b): The two antennas form a perpendicular angle between them (VH or HV).
- (c): The two antennas are in the same plane, but they are perpendicular to the (a) case (VV).
- (d): The two antennas are in the same plane, but they are perpendicular to the (a) case, and they are separated by a metallic plate. We have represented different S_{21} results in Figure 13.

After simulation, we decided to do our measures with case (b) which presented less coupling effect as shown in Figure 13. We note here that in case (d), this technique could give good results, but antennas

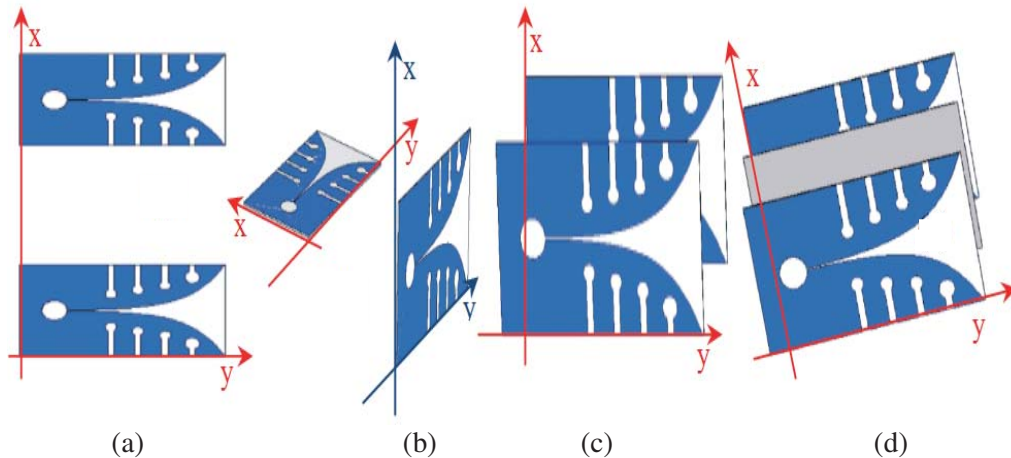


Figure 12. Position of transmitting and receiving antennas: (a) Tx//Rx, (b) $Tx \perp Rx$, (c) $(Tx//Rx) \perp (a)$, (d) Tx//Rx with separator metallic plat.

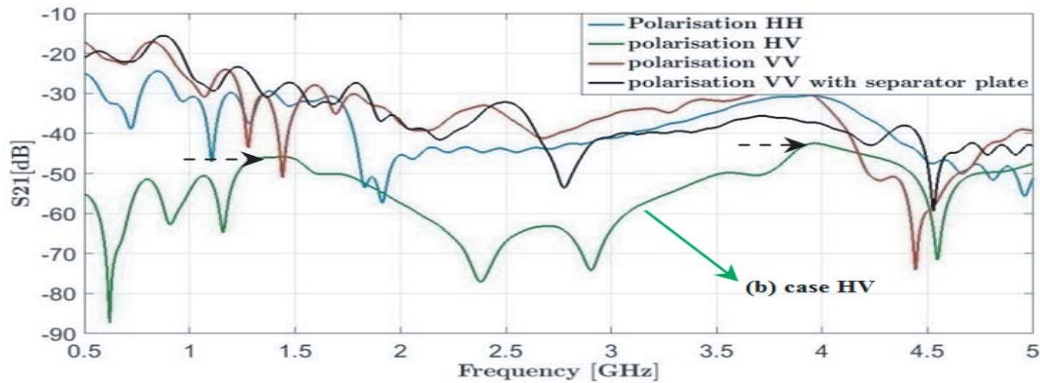


Figure 13. Coupling effect versus different polarizations.

beams would clearly be modified and if we apply SAR technique, because the separator metallic plate did not let the reflected wave by objects reach the receiving antenna [21, 22].

The result showed, in (b-HV) case from Figure 13, a coupling effect lower than -44 dB from 1.4 to 1.5 GHz and lower than -42 dB at 3.9 GHz between two antennas. Hence, we have seen that this polarization gives us the minimum coupling effect considered in our experimental measures.

3. EXPERIMENTAL STUDY AND RESULTS

In order to validate the new designed antenna, measurements were performed in laboratory, in controlled configurations.

The first campaign is carried out using a sandbox, in which some objects are embedded. The constant dielectric of sand is estimated with simple techniques. First, we have used a trihedral corner reflector at a known depth, then we have done one measure by applying the IFT on the S_{21} coefficients to get the antenna origin radiation in the time domain. The second one is to calculate the relative permittivity by optical geometry. The value is estimated to be about 3, 88.

The principle of measurement is to record the S_{21} coefficients for the ultrawide frequency band, on which we apply an Inverse Fourier Transform. For each antenna position, a time signal is then calculated (called Ascan). While moving the antennas, different measurements (Ascan) can be contiguous to have a 2D time slide (Bscan).

Our scans were done manually with a step of 1 cm, and the antennas were at a height of 10 cm from the ground surface. We have registered the radar data from the network analyzer to a computer. By applying the IFT, a B-scan image is obtained.

The experimental measurement device of the GPR in laboratory is shown in Figure 14.

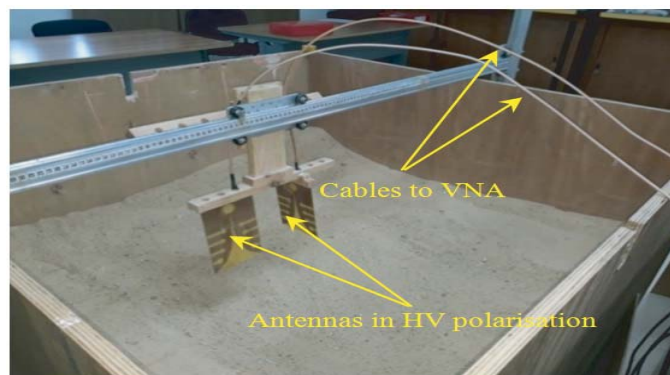


Figure 14. Experimental measurement device of the GPR in laboratory.

According to Figure 15, for example, the targets are two trihedral corner reflectors separating between them with 8 cm from their centers in a depth of 12 cm. This distance can be shown at 27.8 cm which is equivalent to 12 cm when ϵ_r is considered.

SAR technique based on back projection was employed. This technique often requires an array of antenna apertures to look at the targets. A uniform linear array of receiving elements is used for capturing echoes of targets through wall. In our case, we have replaced the case of measure every 1 cm as an echo from a new antenna of a uniform array of antennas. The pair of antenna made scans forms an image (2D-Bscan). Back-projection coherently sums the sampled returns for each antenna position element (pixel) of the image map. By the phrase coherent summation, it means that the signal obtained at each antenna position is time-shifted to match, or align, into a particular pixel element in the image map. Following this, the responses across all aperture positions are combined [18–20].

From Figures 17 and 18, we can easily see the two metallic trihedral corner reflectors at a distance of 1.5 m from the wall; however, plastic targets are not detectable because of their poor reflectivity and strong attenuation of the wall.

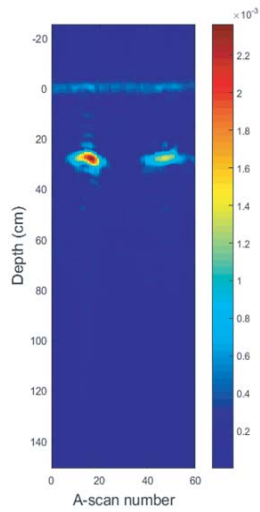


Figure 15. GPR detection using two trihedral corner reflectors.

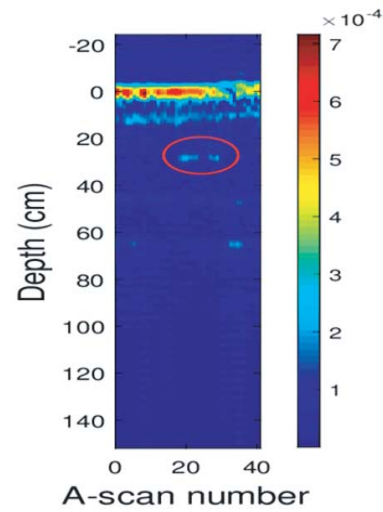


Figure 16. GPR detection using two plastic cylinders.

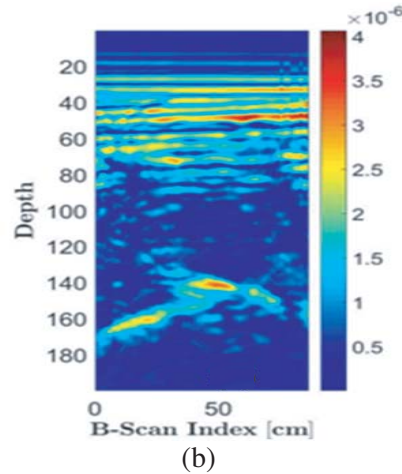
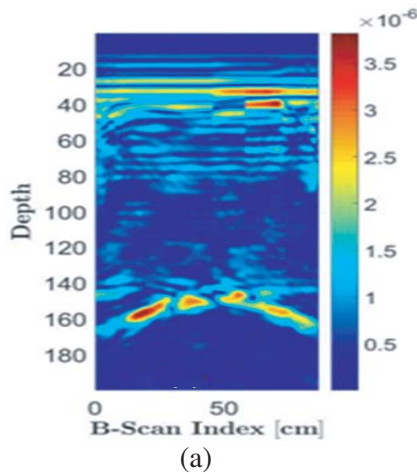


Figure 17. GPR detection of two trihedral corner reflectors in same position through 10 cm wide brick wall in (a) and separated in depth of 15 cm in (b).

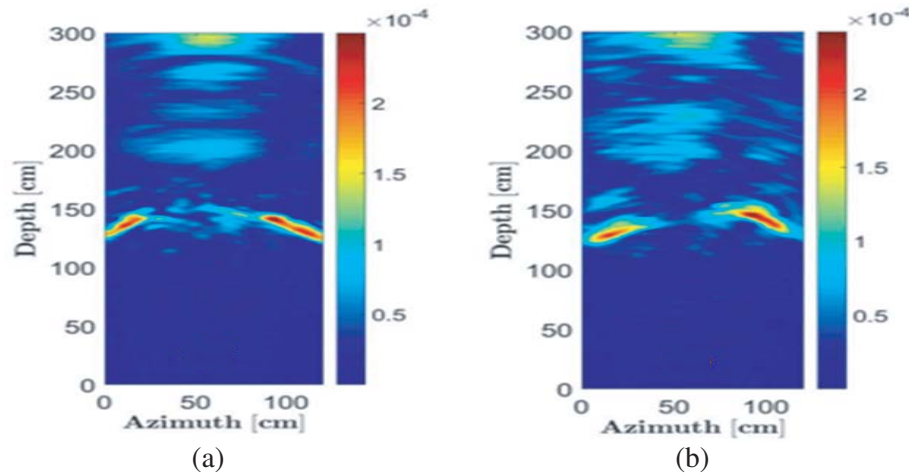


Figure 18. SAR technique applied to GPR data for two trihedral corner reflectors through 10 cm wide brick wall at same position in (a) and separated by 15 cm in depth in (b).

4. CONCLUSION

In this work, we have designed a modified Vivaldi antenna and improved its performances. Simulated and measured results showed satisfactory agreement in the frequency band of 1.17 to 4.75 GHz. The reduction of mutual coupling effect was considered.

The antenna is meant for the use in GPR and through the wall imaging due to its gain and directive beam at its band frequencies. Analysis has shown that the proposed antenna can achieve a better performance of deep penetration of electromagnetic signal to transmit the waves inside soil and through wall efficiency due to its lower frequency of broadband. By applying SAR technique to the measured GPR raw data, it is shown that the method provides focused targets. GPR data were acquired by the help of VNA.

REFERENCES

1. Elsheakh, D. M. N., N. A. Eltresy, and E. A. Abdallah, "Ultra wide bandwidth high gain Vivaldi antenna for wireless communications," *Progress In Electromagnetics Research Letters*, Vol. 69, 105–111, 2017.
2. He, S. H., W. Shan, C. Fan, Z. C. Mo, F. H. Yang, and J. H. Chen, "An improved Vivaldi antenna for vehicular wireless communication system," *IEEE Antennas and Wireless Propagation Letters*, Vol. 13, 1505–1508, 2014.
3. Pandey, G. K., H. S. Singh, P. K. Bharti, A. Pandey, and M. K. Meshram, "High gain Vivaldi antenna for radar and microwave imaging applications," *International Journal of Signal Processing Systems*, Vol. 3, No. 1, Jun. 2015.
4. Bourqui, J., M. Okoniewski, and E. C. Fear, "Balanced antipodal Vivaldi antenna with dielectric director for near-field microwave imaging," *IEEE Transactions on Antennas and Propagation*, Vol. 58, 2318–2326, 2010.
5. Danjuma, I. M., F. Abdussalam, B. Muhammad, E. N. Eya, R. Abd-Alhameed, and J. M. Noras, "Design of a taper slot low profile Vivaldi antenna for ultra-wideband microwave breast imaging applications," *Journal of Multidisciplinary Engineering Science and Technology (JMEST)*, Vol. 4, No. 8, ISSN: 2458-9403, Aug. 2017.
6. Yang, Y., Y. Wang, and A. E. Fathy, "Design of compact Vivaldi antenna arrays for UWB see through wall applications," *Progress In Electromagnetics Research*, Vol. 82, 401–418, 2008.

7. Liu, X., M. Serhir, A. Kameni, M. Lambert, and L. Pichon, "Buried targets detection from synthetic and measured B-scan ground penetrating radar data," *11th European Conference on Antennas and Propagation (EUCAP)*, 1726–1730, 2017.
8. Ali, J., N. Abdullah, M. Y. Ismail, P. Arias, E. Mohd, and S. Mohd Sara, "Ultra-wideband antenna design for GPR applications: A review," *International Journal of Advanced Computer Science and Applications*, Vol. 8, No. 7, 2017.
9. Marpaung, D. H. N. and Y. Lu, "A comparative study of migration algorithms for UWB GPR images in SISO-SAR and MIMO-array configurations," *15th Int. Radar Symposium (IRS 2014)*, 1–4, Gdanskpp, 2014.
10. Dérobert, X., C. Fauchard, Ph. Côte, E. Le Brusq, E. Guillanton, J. Y. Dauvignac, and Ch. Pichot, "Step frequency radar applied on thin road layers," *J. Appl. Geophys.*, Vol. 47, 317–325, 2001.
11. Guan, B., A. Ihamouten, X. Dérobert, D. Guilbert, S. Lambot, and G. Villain, "Near-field full-waveform inversion of ground-penetrating radar data to monitor the water front in limestone," *IEEE Journal of Selected Topics in Applied Earth Observations and Remote Sensing*, Aug. 9, 2017.
12. Lambot, S. and F. Andre, "Full-wave modeling of near-field radar data for planar layered media reconstruction," *IEEE Trans. Geosci. & Remote Sens.*, Vol. 52, 2295–2303, 2014.
13. Gibson, P. J., "The Vivaldi aerial," *9th European Microwave Conference*, 101–105, 1979.
14. Lewis, L. R., M. Fasset, and J. Hunt, "A broad-band strip line array element," *Proc. IEEE Int. Symp. Antennas Propagat. Dig.*, 335–337, 1974.
15. Molaei, A., M. Kaboli, S. A. Mirtaheri, and S. Abrishamian, "Beamtilting improvement of balanced antipodal Vivaldi antenna using a dielectric lens," *Proc. 2nd Iranian Conference on Engineering Electromagnetics*, 577–581, Tehran, Iran, 2014.
16. Dhawan, R. and G. Kaur, "Vivaldi antenna simulation on defining parameters, parametric study and results," *JCTA*, Vol. 9, 5129–5138, 2016.
17. Abbosh, A. M., "Directive antenna for ultra wide band medical imaging systems," *International Journal of Antennas and Propagation*, Vol. 2008, 6 pages, Article ID 854012, 2008.
18. Liu, X., M. Serhir, A. Kameni, M. Lambert, and L. Pichon, "Buried targets detection from synthetic and measured B-scan ground penetrating radar data," *11th European Conference on Antennas and Propagation (EuCAP 2017)*, Paris, France, Mar. 2017.
19. Mostafa, M. A., M. Samir, K. Hussein, and H. Kamel, "SAR processing for buried objects detection using GPR," *Journal of Multidisciplinary Engineering Science and Technology (JMEST)*, Vol. 3, No. 6, ISSN: 2458-9403, Jun. 2016.
20. Marpaung, D. H. N. and Y. Lu, "A comparative study of migration algorithms for UWB GPR images in SISO-SAR and MIMO-array configurations," *15th Int. Radar Symposium (IRS 2014)*, 1–4, Gdanskpp, 2014.
21. Perdana, M. Y., T. Hariyadi, and Y. Wahyu, "Design of Vivaldi microstrip antenna for ultra-wideband radar applications," *IOP Conf. Series: Materials Science and Engineering*, 180, 2017.
22. Ma, K., Z. Zhao, J. Wu, S. M. Ellis, and Z.-P. Nie, "A printed Vivaldi antenna with improved radiation patterns by using two pairs of eye-shaped slots for UWB," *Progress In Electromagnetics Research*, Vol. 148, 63–71, 2014.
23. Frenando, I., R. M. Pereira, H. Lorenzo, P. Arias, and A. Novo, "Resolution of GPR bowtie antennas: An experimental," *Journal of Applied Geophysics*, 367–373, 2009.
24. Wu, Y., J. P. Linnartz, J. W. M. Bergmans, and S. Attallah, "Effects of antenna mutual coupling on the performance of MIMO systems," *Symposium on Information Theory in the Benelux*, May 2008.